Received: 10 February 2023 | Accepted: 12 May 2023

DOI: 10.1002/pc.27435

RESEARCH ARTICLE

Polymer COMPOSITES WILEY

Tailoring the physical properties of poly(lactic acid) through the addition of thermoplastic polyurethane and functionalized short carbon fibers

L. Simonini[1,2] | H. Mahmood[1,2] | A. Dorigato[1,2] | A. Pegoretti[1,2]

[1]Department of Industrial Engineering, University of Trento, Trento, Italy

[2]National Interuniversity Consortium of Materials Science and Technology (INSTM), Florence, Italy

Correspondence
L. Simonini, Department of Industrial Engineering, University of Trento, Via Sommarive 9, 8123 Trento, Italy.
Email: laura.simonini@unitn.it

Abstract

The elevated brittleness of commercial grades of poly(lactic acid) (PLA) may limit their use in several engineering applications. Therefore, the aim of this work is to develop a PLA-based material possessing well-balanced stiffness and toughness. Composites were prepared by blending PLA with increasing contents (from 10 to 30 wt%) of a thermoplastic polyurethane (TPU) and a fixed concentration (5 wt%) of carbon fibers (CFs), to tune the mechanical properties of the resulting materials. In order to increase the interfacial adhesion between CFs and polymeric phase, CFs were subjected to an acidic modification, by treating them in solution of H_2SO_4 and HNO_3. The prepared composites were characterized from a chemical, rheological, morphological, and thermo-mechanical point of view. Fourier transform infrared spectroscopy showed that the fiber surface reactivity was significantly enhanced by the acid treatment, with the introduction of reactive functional groups on CFs. Rheological and dynamic-mechanical tests confirmed that the introduction of acid-treated CFs implied strong fiber–matrix interactions. Thanks to the presence of the acid treated CFs, an important increase in tensile modulus and maximum stress was obtained for all the compositions. In particular, samples containing 10 wt % of TPU showed +74% tensile modulus and +43% maximum stress with respect to the unfilled blends. Moreover, the elongation at break of PLA was significantly improved (+81%) with the addition of 30 wt% of TPU. It was therefore demonstrated that the adopted approach could be effective for the preparation of novel PLA-based materials with tailorable and well-balanced properties that could find application in various technological fields.

KEYWORDS

biopolymers, composites, fibers, functionalization of polymers, interfaces

1 | INTRODUCTION

The urge of replacing petroleum-based polymers is pushing materials engineers toward the development of new products based on natural resources, and biopolymers are therefore receiving growing interest in the scientific community.[1–3] Biopolymers are polymeric materials made starting from renewable resources and/or biodegradable,[4–6] and among them, poly(lactic acid) (PLA) displays interesting physical and mechanical

properties.[7–10] It is a bio-based and biodegradable aliphatic polyester derived from lactic acid. PLA can be either an amorphous, semicrystalline or highly crystalline polymer. Due to the chiral nature of the lactic acid, it can be found either in the form of poly-L-lactide (PLLA) or poly-D-lactide and in the racemic mixture of poly-DL-lactide. It is a relatively cheap polymer and offers excellent degradability and barrier properties.[11] It can be processed in many ways such as extrusion, spinning, or injection molding, with vast application perspectives in the future.[8,12–15] However, PLA is rather brittle, and this feature may limit its application in many industrial segments.[16] Therefore, there is a common interest to formulate new grades of PLA with improved ductility, while maintaining its tensile strength.[17–20] At this aim, different methods have been adopted, such as the use of plasticizers,[21–23] incorporation of fillers,[24–26] and blending with other polymers having elevated ductility.[27–31] In particular, the possibility of blending PLA with elastomers[32,33] and thermoplastic polyurethanes (TPUs)[34–38] has been widely investigated in literature. TPU is a melt-processable thermoplastic elastomer characterized by high durability, flexibility, biocompatibility, and biostability.[39,40] It is produced by the polycondensation reaction between a diisocyanate and one or more diols, thus providing a chemical structure made of soft segments (SS) and hard segments (HS).[41] The SS give flexibility and elastomeric behavior while the HS give stiffness and hardness to the structure. Thanks to its peculiar properties, TPU is used in a variety of applications such as in 3D printing, automotive, medical, and sport sectors.[42–46] For instance, Jašo et al.[47] blended PLA with TPU at different relative ratios, showing that the thermal, morphological, and mechanical properties of PLA were strongly affected by the addition of TPU. Feng and Ye[48] showed that the strength of PLA declined slowly by increasing the TPU content, while the elongation at break was considerably improved for TPU amounts higher than 5 wt%. However, Han and Huang[49] proved that, for a satisfactory toughening of PLA, elevated amounts of TPU (>30 wt%) must be added to PLA. The major drawback of adding large concentrations of TPU is the substantial decrease in strength and elastic modulus. Moreover, also the biodegradability of the resulting blends could be strongly impaired. So, a polylactide-based material at elevated PLA contents with balanced stiffness and toughness is still difficult to be developed. The addition of fillers may help to overcome this problem, thus obtaining a ternary material having better mechanical properties compared with the unfilled blends.[50–53] In this sense, Xiu et al.[54] added hydrophilic silica (SiO_2) nanoparticles to PLA/TPU blends, obtaining a discontinuous network-like morphology that allowed a noticeable improvement in the impact toughness of the blend. In another work, Xiu et al.[55] introduced titanium dioxide (TiO_2) nanoparticles in PLLA/TPU blends, showing that nano-TiO_2 particles selectively localized at the interface and led to a significant improvement in impact toughness. Recently, carbon fibers (CFs) have been considered as an ideal candidate to improve the mechanical properties of polymer blends, thanks to their outstanding strength and stiffness.[3,56–58] In literature, it is reported that CFs can be used as reinforcement to improve the strength of polymers such as PLA and TPU.[59–61] Yin et al.[62] introduced various amounts of CFs in PLA/TPU blends, showing that the addition of CFs tended to decrease the thermal stability, while the tensile strength was increased by about 11.4% with a CF concentration of 10 wt% Qian et al.[63] prepared CF-reinforced PLA/TPU blends, studying the effect of the fiber length and content on the morphological, thermal, rheological, and mechanical properties of the resulting materials. It was shown that the mechanical performances were almost unaffected by the fiber length, while the CFs content strongly influenced the tensile and impact strength of the composites. However, when CFs were used without any surface treatment, the resulting composites possessed low interfacial (IFSS) or interlaminar shear strength (ILSS).[64,65] Inadequate interfacial properties can thus represent a serious problem in these systems.[66–70] In order to overcome this limitation, surface treatments can increase the chemical compatibility of CFs with the matrix.[71] Various methods have been proposed in the literature, such as plasma treatments, gas phase oxidation, heat, and polymerization treatments.[72] Among them, nitric (HNO_3) and sulfuric (H_2SO_4) acid oxidative treatment is an effective method to strengthen the interfacial adhesion properties. This approach enhances the physical and chemical interaction between fibers and matrix, by roughening the CF surface and also introducing reactive functional groups compatible with the polymer matrix.[73] Zhang et al.[74] used H_2SO_4/HNO_3 acid mixtures to functionalize CFs, demonstrating the presence of O-/N-/S-containing groups on CFs surface. Tiwari et al.[75] used HNO_3 to include oxygenated functional groups on the surface of CFs, to enhance the interfacial adhesion with a thermoplastic polyetherimide matrix, obtaining an improvement of the ILSS and the flexural strength of 71% and 29%, respectively.

Based on these considerations, the present work aims to investigate, for the first time, the effect of the oxidative acid treatment (H_2SO_4/HNO_3) of CFs surface on the mechanical performances of PLA/TPU/CF composites. The morphological and chemical properties of CFs before and after the surface modification were systematically investigated. Both untreated and acid-treated CFs were then added to PLA/TPU blends, and a comprehensive rheological, morphological, thermal, and mechanical characterization of these ternary composites was

performed. In this way, it could be possible to obtain PLA based composites with tailorable mechanical properties that could overcome the actual technological limits of PLA and could extend the application fields of this material.

2 | EXPERIMENTAL PART

2.1 | Materials

Pellets of PLA (density = 1.24 g/cm^3, MFI at 210°C and 2.16 kg = 7 g/10 min, product code 4032D) were purchased by NatureWorks LLC (Minnetonka, USA). Pellets of TPU (density = 1.23 g/cm^3, melting temperature range 220–240°C, product code 3059D) was supplied by Covestro Srl (Milano, Italy). Chopped CFs Panex PX35 type 65 (density = 1.81 g/cm^3), having an average length of 6 mm and a mean diameter of 8 μm, were provided by Xenia Materials Srl (Vicenza, Italy). Sulfuric acid (H_2SO_4, purity 96%) and nitric acid (HNO_3, purity 69%) were provided by Sigma Aldrich (Saint Louis, MO, USA).

2.2 | Sample preparation

2.2.1 | Functionalization of carbon fibers surface

Following the procedure described in Reference 74, acid treatment of CFs was performed by immersing them in a H_2SO_4/HNO_3 acid mixture (relative weight ratio 3:1) under ultrasonic treatment. The treatment was performed for 15 min at 60°C using a FALC (Shenzhen, China) ultrasonic bath. Then, the fibers were washed at room temperature under continuous stirring in deionized water to reach a neutral pH, and then dried at 80°C for 24 h under vacuum. In this work, untreated CFs were designed as uCF, while treated (functionalized) CFs were denoted as fCF.

2.2.2 | Composite preparation

Initially, both the polymers and the fibers were dried at 50°C for at least 72 h. PLA, TPU and CF were melt compounded in a Thermo Haake Rheomix® 600 internal mixer at 220°C for 5 min, setting a rotor speed of 50 rpm. Then, the resulting compounds were compression molded at 220°C for 5 min at a pressure of 3.4 MPa, thus obtaining rectangular sheets with dimensions of 120 × 120 × 1 mm^3. The samples were prepared according to the formulations listed in Table 1.

2.3 | Experimental techniques

CFs were characterized by Fourier transform infrared (FTIR) spectroscopy in attenuated total reflectance mode with a Perkin Elmer Spectrum One FTIR spectrometer (Perkin Elmer, USA). A minimum of 16 scans with a resolution of 4 cm^{-1} were performed, between a scanning interval of 4000 and 650 cm^{-1}.

The dynamic rheological properties of the composite samples were analyzed through a Discovery Hybrid Rheometer (DHR-2) (TA Instruments, USA), by adopting a plate-plate configuration. These tests were carried out at 220°C, applying a strain amplitude of 1% on discoidal specimens with a diameter of 25 mm. The thickness of the gap was set at 1 mm. In this way, the trends of the storage modulus (G'), of the loss modulus (G''), and of the complex viscosity (η) were investigated in an angular frequency (ω) range between 0.1 and 100 rad/s.

The morphological observations were performed through a Zeiss Supra 40 field-emission scanning electron microscope, operating at an acceleration voltage of 3.5 kV.

TABLE 1 List of the prepared PLA/TPU/CF composites.

Sample	PLA (wt%)	TPU (wt%)	uCF (wt%)	fCF (wt%)
PLA	100.0	–	–	
PLA/10	90.0	10.0	–	
PLA/20	80.0	20.0	–	
PLA/30	70.0	30.0	–	
PLA/10/uCF	85.5	9.5	5.0	
PLA/20/uCF	76.0	19.0	5.0	
PLA/30/uCF	66.5	28.5	5.0	
PLA/10/fCF	85.5	9.5	–	5.0
PLA/20/fCF	76.0	19.0	–	5.0
PLA/30/fCF	66.5	28.5	–	5.0

Before the observation, the samples were coated with a Pt/Pd alloy (80:20) conductive layer having a thickness of about 5 nm.

Differential scanning calorimetry (DSC) was performed by using a Mettler DSC30 calorimeter (Mettler Toledo, Columbus, OH). The samples were heated from 0 to 200°C and subsequently cooled from 200 to 0°C. Finally, a second heating stage was applied from 0 to 200°C. These thermal ramps were performed at a rate of 10°C/min, under a nitrogen flux equal to 100 mL/min. Only one specimen was tested for each composition. The relative degree of crystallinity (χ) of the PLA phase in the samples was calculated through Equation (1).

$$\chi = \frac{\Delta H_m - \Delta H_{cc}}{\varphi_{PLA}\,\Delta H_m^0} \times 100, \quad (1)$$

where ΔH_m is the enthalpy of fusion of PLA, ΔH_{cc} is the enthalpy of cold crystallization of PLA, φ_{PLA} is the weight fraction of PLA in the composite, and ΔH_m^0 is the standard melting enthalpy of the fully crystalline PLA, taken as 93.7 J/g.[76]

Thermogravimetric analysis (TGA) was carried out by using a TA-IQ5000 IR (New Castle, USA) thermobalance under an air flow of 100 mL/min in a temperature interval from 35 to 700°C at a heating rate of 10°C/min. The onset of degradation temperature (T_{onset}), the degradation temperature (T_d) corresponding to the temperature associated to the maximum mass loss rate, and the residual mass (m_{700}) at the end of the tests were determined.

Dynamic mechanical analysis (DMA) was carried out in tensile mode by using a TA Q800DMA (TA Instruments, USA) machine. Rectangular specimens (30 × 5 × 1 mm^3) with a gage length of 10 mm were tested in a temperature range from 0 to 200°C at a heating rate of 3°C/min, a test frequency of 1 Hz, a strain amplitude of 0.05%. In this way, the trends of the storage modulus (E'), of the loss modulus (E''), and of the loss tangent (tanδ) were investigated as a function of temperature. The glass transition temperature (T_g) of the PLA phase was estimated from the tanδ peak.

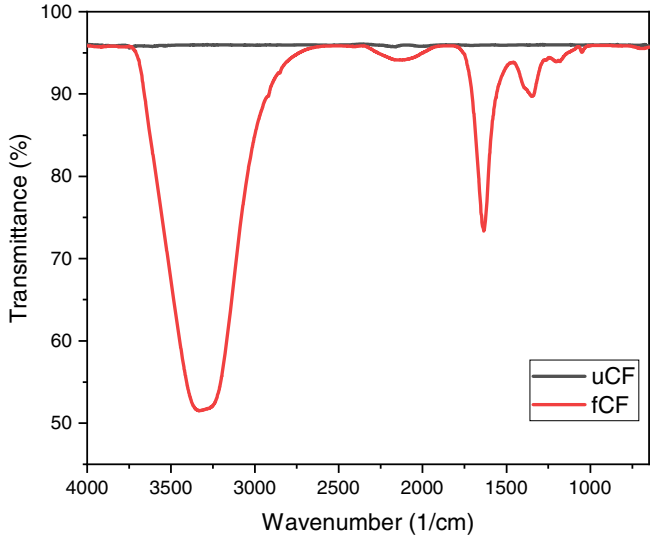

FIGURE 1 FTIR spectra of CFs before (uCF) and after (fCF) the acid treatment.

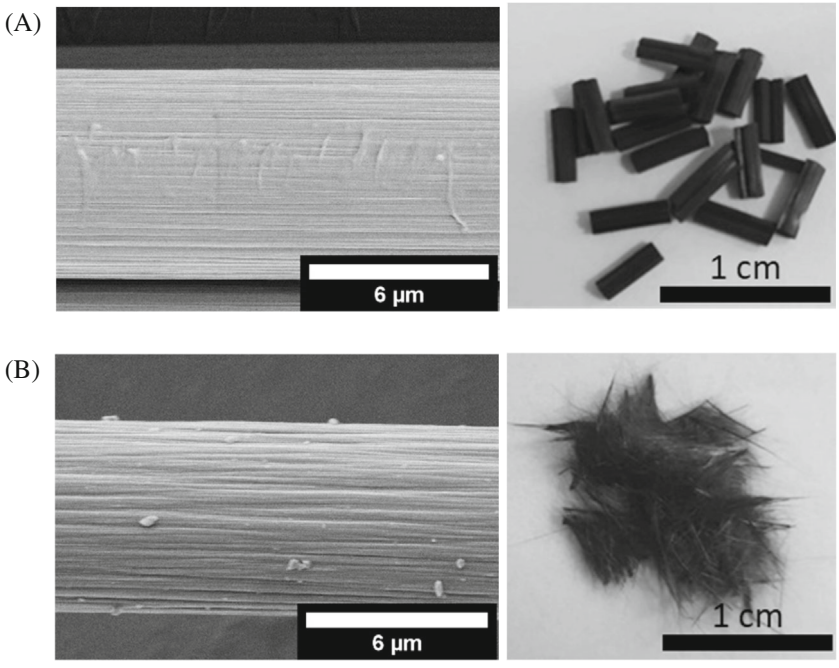

FIGURE 2 SEM micrographs of (A) uCF and (B) fCF, together with their optical appearance.

Quasi-static tensile tests were performed by using an Instron® 5969 (Instron, USA) universal testing machine, equipped with a load cell of 1 kN, testing 1BA type dumbbell specimens according to the ISO 527 standard. Tensile tests for the evaluation of the elastic modulus (E) were performed at a crosshead speed of 0.25 mm/min, imposing a maximum axial deformation level of 1%. The strain was recorded by using a dynamic extensometer Instron model 2620-601 (gauge length of 12.5 mm). According to ISO 527 standard, the elastic modulus was evaluated as a secant value between deformation levels of 0.05% and 0.25%. Tensile properties at break were evaluated at a crosshead speed of 1 mm/min, without using the extensometer. The maximum stress (σ_{max}) and the elongation at break ($\epsilon_{\%}$) were determined for each composition. At least five specimens were tested for each sample.

3 | RESULTS AND DISCUSSION

3.1 | Chemical and morphological characterization of carbon fibers

FTIR spectroscopy allowed to detect the functional groups introduced on the surface of the fibers by the acidic treatment. Figure 1 shows the FTIR spectra of CFs before and after the acid treatment. Strong absorption bands of –OH groups appear at 3332 cm^{-1} after the chemical modification of CFs. The bands around 1300 and 1700 cm^{-1} correspond to the stretching vibrations of –C═O group. Similar FTIR transmittance spectra of CFs before and after an acidic treatment can be found in literature.[77,78] These observations confirm that the fiber surface activity was significantly enhanced by the acidic

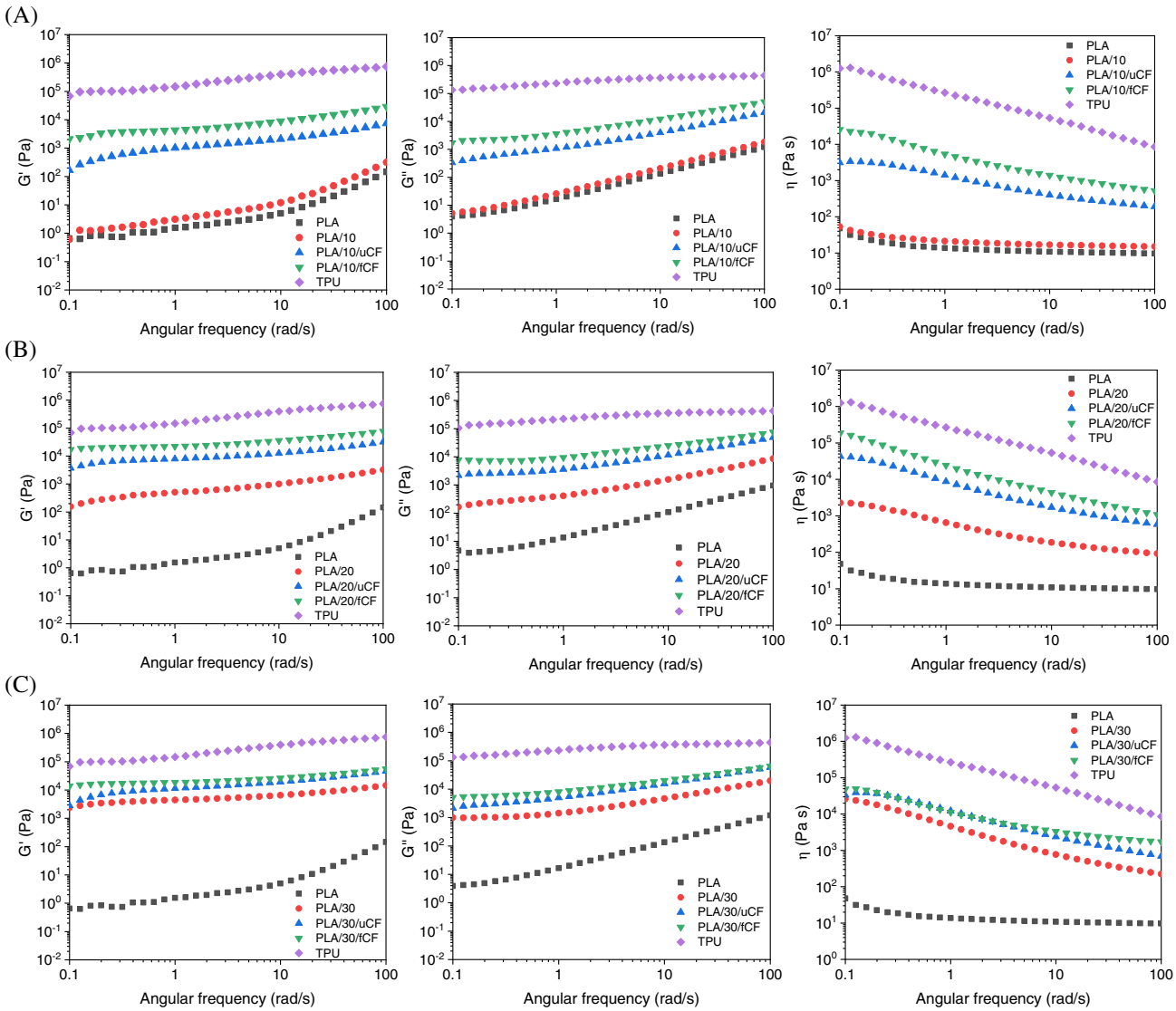

FIGURE 3 Storage modulus (G'), loss modulus (G''), and complex viscosity (η) of neat PLA and TPU, of the blends and of the relative composites. TPU content of (A) 10 wt%, (B) 20 wt%, and (C) 30 wt%.

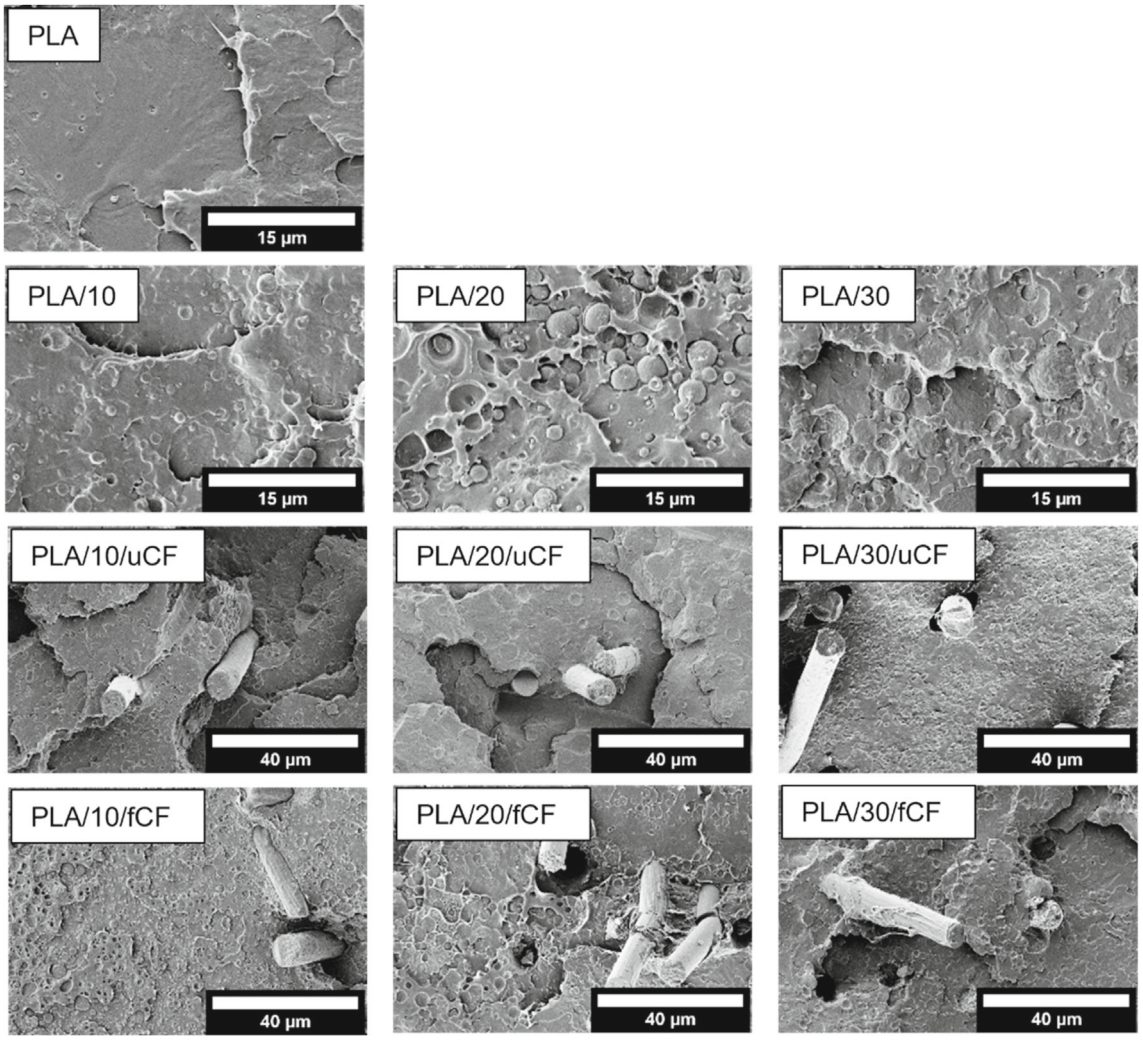

FIGURE 4 SEM micrographs of PLA, PLA/TPU blends, and their relative composites.

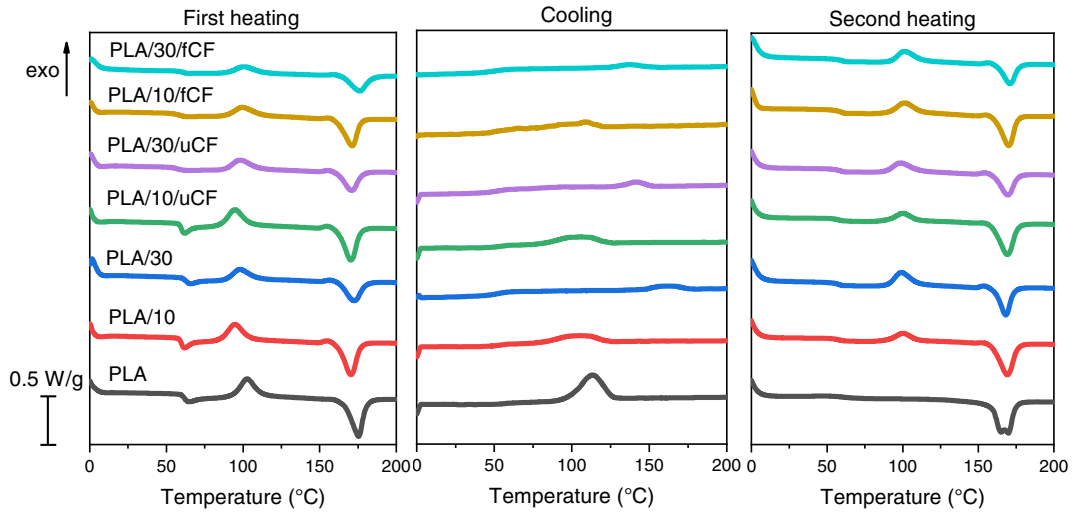

FIGURE 5 DSC thermograms of neat PLA, PLA/TPU blends, and the relative composites.

treatment, which introduced reactive functional groups on the CF surface.

SEM micrographs of uCF and fCF are represented in Figure 2A,B, together with their optical appearance. The surface of the fibers results to be altered after the chemical modification, as the fCFs seem considerably rougher than uCFs. The presence of deeper groves increases the surface area of fCF, thus improving the number of active sites on the fiber surface. These sites could provide a better mechanical interlocking between CFs and the polymeric phases, ultimately increasing the interfacial adhesion.[75,78] Moreover, the chemical modification of CFs tends to separate the short fibers from the bundles, making their dispersion inside the matrix easier during melt compounding.

3.2 | Rheological characterization of the composites

Figure 3A–C shows the dynamic rheological properties of neat PLA and TPU, of their blends and of the relative composites in terms of storage modulus (G'), loss modulus (G''), and complex viscosity (η).

At a general level, it can be noticed that all the samples present a pseudoplastic behavior, with a decrease of the complex viscosity as a function of the frequency. It can be also concluded that the TPU matrix has higher G', G'', and η values with respect to PLA. Therefore, the dynamic moduli and the viscosity of PLA/TPU blends increase with the TPU amount. This trend can be also partially due to the formation of hydrogen bonds between the carbonyl groups of TPU and the hydroxyl groups of PLA, and the subamide groups of TPU and the carboxyl group of PLA.[79] As it could be expected, regardless of the TPU content, the presence of CFs in the blends shifts the rheological parameters to higher values, because the chain mobility is restricted by the fibers. Considering the composites with the same CF concentration, it can be noticed that the G', G'', and η values of fCFs filled samples are systematically higher than that of the samples containing uCFs. Higher viscosity implies a stronger fiber–matrix interaction, and this means that the acidic treatment on CFs probably leads to a stronger interfacial bonding with the PLA/TPU matrix.

3.3 | Morphological characterization of the composites

SEM micrographs of neat PLA, PLA/TPU blends and the relative composites are represented in Figure 4. PLA exhibits a relatively smooth and clear surface, typical of a brittle polymer. In the micrographs of the blends, it is

TABLE 2 Results of DSC tests on neat PLA, PLA/TPU blends, and the relative composites.

	First heating					Cooling		Second heating				
	T_g (°C)	T_{cc} (°C)	T_m (°C)	ΔH_{cc} (J/g)	ΔH_m (J/g)	χ (%)	T_c (°C)	ΔH_c (J/g)	T_g (°C)	T_{cc} (°C)	T_m (°C)	ΔH_{cc} (J/g)	ΔH_m (J/g)	χ (%)
PLA	61.0	102.9	173.8	36.2	46.7	11.2	114.3	44.3	58.7	–	168.1	–	52.7	56.2
PLA/10	59.1	94.7	168.5	29.8	40.1	12.2	106.1	18.1	56.7	99.7	167.4	14.7	42.6	33.1
PLA/20	60.6	97.6	174.4	23.0	31.0	10.7	179.4	3.0	57.3	99.9	167.3	22.9	32.5	12.9
PLA/30	61.7	97.7	171.7	20.8	26.1	8.1	162.7	6.9	56.9	99.1	167.0	22.6	25.9	5.0
PLA/10/uCF	57.9	99.5	169.8	25.4	32.9	9.4	109.3	11.3	59.2	100.8	168.8	24.1	34.7	13.2
PLA/20/uCF	59.8	95.8	169.5	19.6	29.9	14.5	147.5	5.3	57.4	98.3	167.8	18.8	30.6	16.6
PLA/30/uCF	55.9	97.8	169.6	19.8	23.6	6.1	142.0	5.8	57.3	98.2	159.0	16.5	26.5	16.0
PLA/10/fCF	60.4	101.5	173.8	20.5	33.6	16.4	113.3	1.1	59.1	104.3	168.9	28.2	32.0	4.7
PLA/20/fCF	59.3	100.4	171.9	19.7	26.3	9.3	135.6	1.1	59.6	102.7	162.2	20.4	25.0	6.5
PLA/30/fCF	60.2	100.3	175.2	15.0	23.2	13.2	138.1	4.1	59.2	101.2	161.6	17.2	23.0	9.3

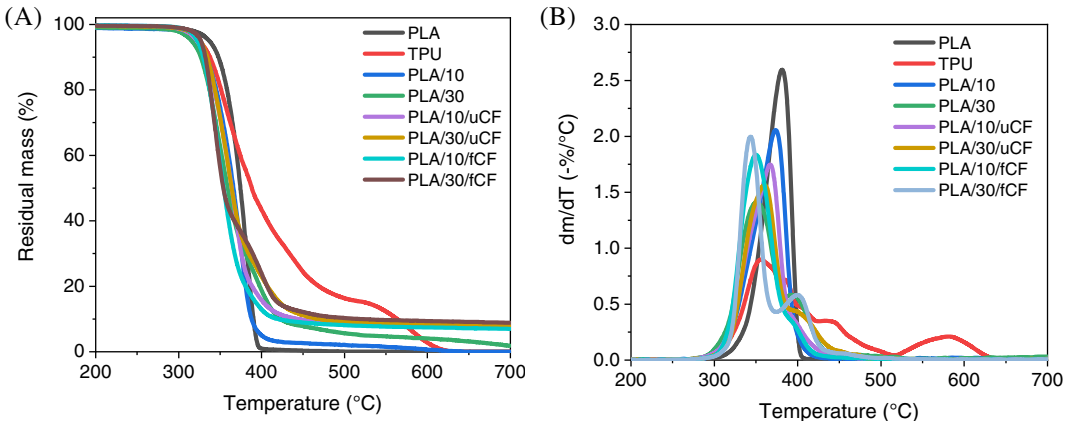

FIGURE 6 Representative TGA thermograms of the prepared samples. (A) Residual mass and (B) mass loss derivative as a function of temperature.

TABLE 3 Results of TGA tests on neat polymers, blends, and the relative composites.

	T_{onset} (°C)	$T_{d,\ PLA}$ (°C)	$T_{d,\ TPU}$ (°C)	m_{700} (%)
PLA	342.3	382.5	–	0.0
TPU	320.2	352.2	433.7	0.0
PLA/10	324.2	369.2	–	0.0
PLA/20	323.9	362.5	–	0.0
PLA/30	320.5	360.2	–	0.0
PLA/10/uCF	330.4	366.8	–	7.9
PLA/20/uCF	330.1	363.0	399.7	6.7
PLA/30/uCF	333.3	360.2	400.7	8.1
PLA/10/fCF	329.7	345.2	–	5.9
PLA/20/fCF	333.4	348.0	391.8	7.0
PLA/30/fCF	326.5	343.3	415.2	8.8

possible to notice that the TPU phase is well dispersed within the PLA matrix, and it assumes a spherical form. However, particle debonding denotes a poor interfacial adhesion between the two phases. By increasing the amount of TPU, their domains become larger in diameter, passing from 1.5 ± 0.5 μm for PLA/10 blend up to 3.9 ± 1.3 μm for the PLA/30 sample. Moreover, the interfacial adhesion with PLA seems to be better when the TPU content increases. Once again, this can be explained by the formation of H-bonds and dipolar interactions between ester and urethane fragments. A similar microstructural behavior is reported in literature for PLA/TPU blends.[62] Analyzing the microstructure of PLA/TPU blends reinforced with uCF, it can be noticed that crack propagation occurs at different planes of the matrix, with failure progressing along the fiber/matrix interface, hence a fiber pull-out phenomenon occurs in such composites. On the contrary, in the blends reinforced with fCF, the fracture plane is almost flat and shorter fiber length can be detected. This indicates a strong interfacial adhesion between the blends and the fibers, which results in the fracture of fibers rather than a fiber pull-out failure mechanism. The reactive groups introduced on the surface of fCFs by the acidic treatment react with the PLA/TPU matrix, thus improving the interfacial adhesion. In addition, some residues of PLA/TPU matrix can be observed along the pulled fCFs, proving once again a better interfacial compatibility with respect to uCFs filled composites.

3.4 | Thermal characterization of the composites

Figure 5 shows the most significant DSC thermograms of the investigated samples, collected during the first heating scan, the cooling, and the second heating scan. The most important results are summarized in Table 2. All the thermal transitions reported in these thermograms

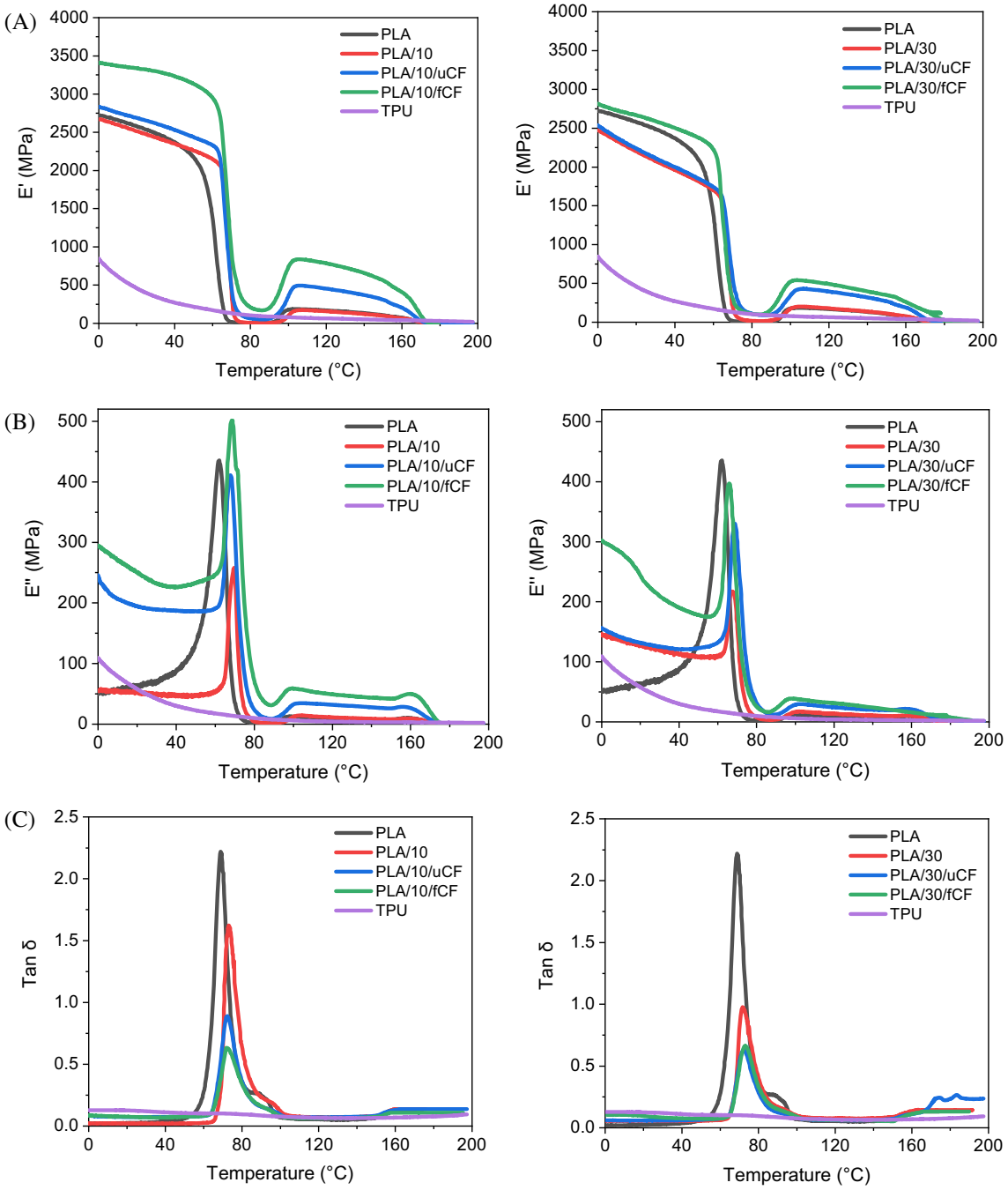

FIGURE 7 DMA tests on neat PLA and TPU, blends, and on the relative composites. Trends of (A) storage modulus (E'), (B) loss modulus (E''), and (C) tanδ at different TPU contents.

are referred to the PLA phase since TPU does not manifest significant transitions in the investigated temperature interval.

The neat PLA has a semicrystalline nature, and it is characterized by a glass transition temperature (T_g) of 61.0°C, a cold crystallization temperature (T_{cc}) of 102.9°C, and melting temperature (T_m) of 173.8°C, taken from the first heating scan. The second heating scan does not present cold crystallization phenomena but indicates a more pronounced melting peak, associated with a higher crystallinity degree. The addition of increasing amounts of TPU and CFs does not lead to substantial changes in the values of T_g, and T_m of the polymer. Instead, both uCFs and fCFs contribute to a slight decrease in the cold crystallization temperature of PLA, since the fiber surfaces may act as nucleating sites. Regarding the χ values, in the first heating scan the degree of crystallinity of PLA seems not to be

	E' (0°C) (MPa)	E' (105°C) (MPa)	tanδ peak intensity	T_g [a] (°C)
PLA	2726	185	2.2	68.4
TPU	844	75	–	–
PLA/10	2672	171	1.6	72.8
PLA/30	2475	202	1.0	73.9
PLA/10/uCF	2835	494	0.9	74.2
PLA/30/uCF	2534	428	0.7	75.7
PLA/10/fCF	3412	838	0.6	73.4
PLA/30/fCF	2814	540	0.6	72.7

[a]Evaluated as the temperature corresponding to the tanδ peak.

TABLE 4 Results of dynamic-mechanical analysis (DMA) on neat polymers, blends and on the relative composites.

substantially affected by the presence of TPU, while in the second heating scan a strong reduction of the χ values is registered. This phenomenon may arise from the ordering of the SS and HS of TPU after the first heating and the cooling steps.[80]

The thermal stability of neat polymers, PLA/TPU blends and the relative composites was investigated by TGA analysis. Figure 6A,B shows the most representative TGA thermograms of the prepared samples in terms of residual mass and mass loss derivative as a function of temperature.

In Table 3, the values of onset degradation temperature (T_{onset}), degradation temperature (T_d), and residual mass (m_{700}) are summarized.

Neat PLA starts to degrade at 342.3°C, reaching a maximum degradation rate at 382.5°C. No residual mass can be found at the end of the thermal treatment. TPU presents an anticipated degradation that starts at 320.2°C, with the maximum degradation rate at 352.2°C. From the first derivative of the TGA curve (Figure 6B), a second degradation peak can be observed for TPU at 433.7°C. As explained in literature, the first degradation step is due to the dissociation of the urethane bonds in the TPU hard segment, while the second degradation step is due to the thermal decomposition of the SS.[81] Regarding the addition of TPU to PLA, the thermal stability of PLA is decreased by increasing the amount of TPU, shifting the onset of degradation and the maximum degradation rate to lower temperatures. In addition, the addition of both untreated and treated CFs results in a decrease of the thermal stability of PLA/TPU composites. This trend was observed also by Yin et al.[62] where the introduction of 5 wt% CF in PLA/TPU matrix decreased the T_{onset} by 22.9°C and $T_{d,PLA}$ by 59.5°C. However, the observed drop does not substantially compromise the applicability of PLA in the packaging field. Moreover, a residual mass at the end of the test is present, due to the incomplete thermal degradation of the CFs in the temperature range analyzed.

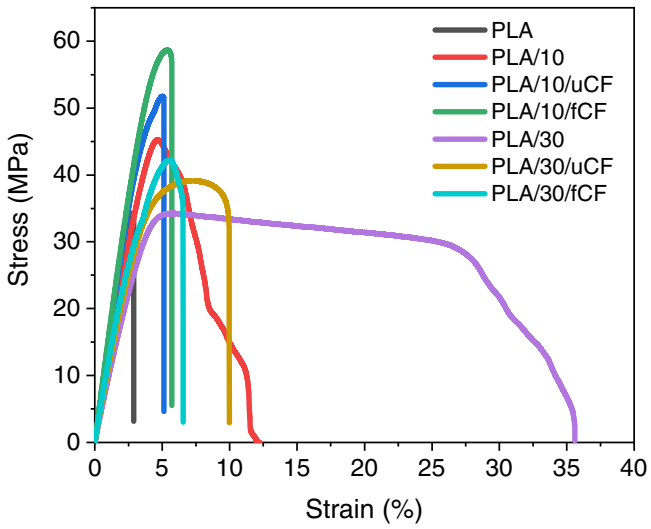

FIGURE 8 Representative stress–strain curves of neat PLA, PLA/TPU blends, and the relative composites.

3.5 | Mechanical characterization of the composites

Dynamic mechanical thermograms of neat PLA and TPU, PLA/TPU blends and the relative composites are represented in Figure 7A–C, while the most important parameters are summarized in Table 4.

The storage modulus (E') of PLA at 0°C is equal to 2726 MPa and it decreases significantly above its T_g (68.4°C). Then, a slight increase of E' up to 185 MPa can be detected between 100 and 160°C, due to the cold crystallization of PLA during the test. TPU shows limited E' values (844 MPa at 0°C) in the temperature range analyzed, since it is above its T_g (−42°C according to the datasheet). Regarding the blends, a slight positive shift in the T_g values is observed upon TPU addition, probably because DMA has a higher sensitivity than DSC in detecting the thermal transitions within the polymeric materials. Moreover, the E' value of PLA decreases with

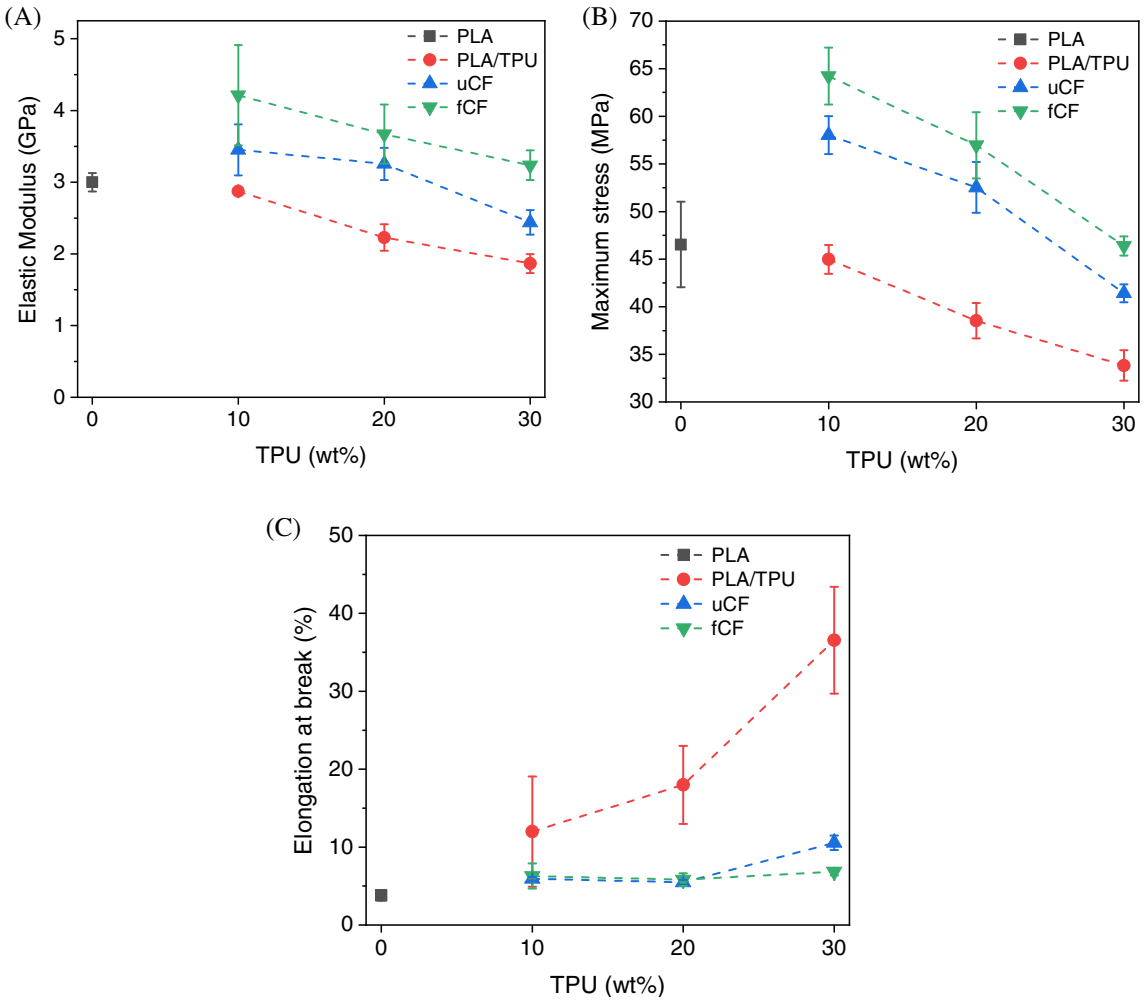

FIGURE 9 Values of (A) elastic modulus, (B) maximum stress, and (C) elongation at break from tensile tests on neat PLA, PLA/TPU blends, and the relative composites.

TPU content and this phenomenon is more evident for sample PLA/30 that shows a decrease of E' of 10% than neat PLA, at 0°C. The introduction of uCFs causes a slight increment of E' below T_g, while a more considerable enhancement can be detected in the case of fCFs (up to 25.2% for PLA/10/fCF at 0°C). Bindu and Thomas[82] showed that this behavior is a clear indication of both a homogeneous dispersion of the reinforcement in the matrix and of the existence of a strong interfacial interaction. The tanδ peaks intensity is reduced in presence of fCF which is also an indication of the improved interaction between the matrix and fCFs: this proofs once again the efficacy of the acid functionalization of CFs.[83] As explained by Chua,[84] the formation of strong bonds between fibers and matrix reduces the motion of the polymeric chains, thus resulting in lower tanδ peak values.

Representative stress–strain curves of neat PLA, PLA/TPU blends, and the relative composites are reported in Figure 8, while the values of elastic modulus, stress at break, and elongation at break are compared in Figure 9A,C.

Neat PLA has an elastic modulus of 3 GPa, a maximum stress of 47 MPa and an elongation at break of 4%. The addition of increasing amounts of TPU (from 10 to 30 wt%) decreases the stiffness and the strength of PLA. In particular, when 30 wt% TPU is added to PLA, the elastic modulus decreases by 38% and the stress at break by 27%. On the other hand, TPU addition leads to a noticeable increase in the elongation at break (up to 867% with a TPU concentration of 30 wt%), highlighting the role played by TPU as toughening agent inside the brittle PLA matrix. The loss of stiffness and maximum stress of PLA is efficiently recovered, and in some cases overcompensated, by the introduction of CFs inside the polymeric matrix, and this beneficial effect is more evident in the case of the fCFs. In particular, due to the addition of 5 wt% fCFs to PLA/10 sample, the elastic

modulus is increased by 47% with respect to the corresponding blend, and only by 20% in the case of uCFs. For PLA/20 blend, the addition of fCFs improves the elastic modulus by 65% (46% for uCF), while for PLA/30 blend by 74% (31% for uCF). Regarding the maximum stress, the introduction of 5 wt% fCF in PLA/10, PLA/20, and PLA/30 samples improves the maximum stress of the corresponding blends by 43%, 48%, and 37%, respectively (29%, 36%, and 22% for uCF). These results suggest that fCFs have a good interfacial compatibility with PLA/TPU matrix, due to the formation of a strengthened interphase upon the acid functionalization of CFs. Regarding the elongation at break, the strong increase given by the introduction of TPU in the PLA matrix is lost by adding both uCFs and fCFs. However, PLA/10/fCF, PLA/20/fCF, and PLA/30/fCF still show higher elongation at break values than neat PLA, with a relative improvement of 66%, 55%, and 81%, respectively. For a given fiber content, the elongation at break values obtained with the introduction of fCF and uCF are quite similar, thus suggesting that the adopted chemical treatment does not substantially influence the elongation at break of the material. It can be therefore concluded that the adopted approach, based on a combination of TPU blending and the addition of functionalized CFs, can lead to an improvement of the stiffness and of the maximum stress of the PLA, and also the ductility of the material is improved. This strategy could represent a valuable solution to extend the application fields of PLA.

4 | CONCLUSIONS

In this work, a PLA matrix was melt compounded with different amounts of TPU and a fixed concentration of CFs, in order to increase the ductility of PLA and to retain its stiffness and strength, with the aim to extend the applicability of this material. Both untreated and functionalized CFs were utilized. Acid surface modification of chopped CFs was performed by dipping the CFs in solution of H_2SO_4 and HNO_3 and performing ultrasonication. Infrared spectroscopy revealed the formation of strong chemical functionalities on the surface of the fibers upon acid treatment. Morphological analysis showed that the fCFs had a rougher surface than uCFs, which allowed a better adhesion with the matrix. Rheological measurements on the composites demonstrated that the introduction of fCFs implied higher complex viscosity values with respect to the composites filled with uCFs, due to a stronger fiber–matrix interaction. DSC and TGA tests showed that the presence of modified fibers did not alter significantly the thermal properties of the PLA matrix. Dynamic-mechanical analysis showed the improved dynamic-tensile properties of composites made of fCFs below T_g and confirmed the enhanced interfacial adhesion between fibers and matrix (see the reduced intensity of tanδ peaks). Quasi-static tensile tests proved that composites made by fCFs showed higher tensile modulus and maximum stress than the corresponding blends, but the introduction of CFs resulted in a drastic reduction of elongation at break with respect to the corresponding blends. However, fCF filled composites still showed improved values of the elongation at break than neat PLA (+81% in the case of PLA/30/fCF). The adopted approach could therefore represent a valuable solution to obtain PLA based composites with tailorable properties, in order to overcome the actual technological limits of PLA and to extend the application fields of this emerging material.

DATA AVAILABILITY STATEMENT

The data that support the findings of this study are available from the corresponding author upon reasonable request.

ORCID

L. Simonini https://orcid.org/0000-0003-3324-7571
A. Pegoretti https://orcid.org/0000-0001-9641-9735

REFERENCES

1. Van de Velde K, Kiekens P. Biopolymers: overview of several properties and consequences on their applications. *Polym Test*. 2002;21:433-442.
2. Schnepp Z. Biopolymers as a flexible resource for nanochemistry. *Angew Chem Int Ed*. 2013;52:1096-1108.
3. Dong K, Panahi-Sarmad M, Cui Z, Huang X, Xiao X. Electro-induced shape memory effect of 4D printed auxetic composite using PLA/TPU/CNT filament embedded synergistically with continuous carbon fiber: a theoretical & experimental analysis. *Compos Part B Eng*. 2021;220:108994-109005.
4. Hall AR, Geoghegan M. Polymers and biopolymers at interfaces. *Rep Prog Phys*. 2018;81:1-37.
5. Dintcheva NT, D'Anna F. Anti-/pro-oxidant behavior of naturally occurring molecules in polymers and biopolymers: a brief review. *ACS Sustain Chem Eng*. 2019;7:12656-12670.
6. Lee N-K. Dynamics and kinetics of polymers and biopolymers. *J Korean Phys Soc*. 2018;73:488-503.
7. Murariu M, Dubois P. PLA composites: from production to properties. *Adv Drug Deliv Rev*. 2016;107:17-46.
8. Ilyas RA, Sapuan SM, Harussani MM, et al. Polylactic acid (PLA) biocomposite: processing, additive manufacturing and advanced applications. *Polymers*. 2021;13:1326.
9. McKeown P, Jones MD. The chemical recycling of PLA: a review. *Sustain Chem*. 2020;1:1-22.
10. Rigotti D, Checchetto R, Tarter S, et al. Polylactic acid-lauryl functionalized nanocellulose nanocomposites: microstructural, thermo-mechanical and gas transport properties. *Express Polym Lett*. 2019;13:858-876.

11. Rigotti D, Fambri L, Pegoretti A. Bio-composites for fused filament fabrication: effects of maleic anhydride grafting on poly(lactic acid) and microcellulose. *Prog Addit Manuf*. 2022;7:765-783.
12. Fredi G, Karimi Jafari M, Dorigato A, et al. Multifunctionality of reduced graphene oxide in bioderived polylactide/poly(dodecylene furanoate) nanocomposite films. *Molecules*. 2021;26:2938.
13. Fredi G, Dorigato A, Bikiaris DN, Checchetto R, Pegoretti A. Furanoate polyesters/polylactide/reduced graphene oxide nanocomposite films: thermomechanical and gas permeation properties. *Macromol Symp*. 2022;405:2100208.
14. Fredi G, Dorigato A, Dussin A, et al. Compatibilization of polylactide/poly(ethylene 2,5-furanoate) (PLA/PEF) blends for sustainable and bioderived packaging. *Molecules*. 2022;27:6371.
15. Rigotti D, Soccio M, Dorigato A, et al. Novel biobased polylactic acid/poly(pentamethylene 2,5-furanoate) blends for sustainable food packaging. *ACS Sustain. Chem. Eng*. 2021;9:13742-13750.
16. Liu H, Zhang J. Research progress in toughening modification of poly(lactic acid). *J Polym Sci B*. 2011;49:1051-1083.
17. Azadi M, Dadashi A, Dezianian S, Kianifar M, Torkaman S, Chiyani M. High-cycle bending fatigue properties of additive-manufactured ABS and PLA polymers fabricated by fused deposition modeling 3D-printing. *Forces Mech*. 2021;3:100016.
18. da Silva Barbosa Ferreira E, Luna CBB, Siqueira DD, Araújo EM, de França DC, Wellen RMR. Annealing effect on pla/eva blends performance. *J Polym Environ*. 2021;30:541-554.
19. Gigante V, Canesi I, Cinelli P, Coltelli MB, Lazzeri A. Rubber toughening of polylactic acid (PLA) with poly(butylene adipate-*co*-terephthalate) (PBAT): mechanical properties, fracture mechanics and analysis of ductile-to-brittle behavior while varying temperature and test speed. *Eur Polym J*. 2019;115:125-137.
20. Koh JJ, Zhang X, He C. Fully biodegradable poly(lactic acid)/-starch blends: a review of toughening strategies. *Int J Biol Macromol*. 2018;109:99-113.
21. Tee YB, Talib RA, Abdan K, Chin NL, Basha RK, Yunos KFM. Toughening poly(lactic acid) and aiding the melt-compounding with bio-sourced plasticizers. *Agric Agric Sci Procedia*. 2014;2:289-295.
22. Meesorn W, Calvino C, Natterodt JC, Zoppe JO, Weder C. Bio-inspired, self-toughening polymers enabled by plasticizer-releasing microcapsules. *Adv Mater*. 2019;31:1807212.
23. Yang Y, Zhang L, Xiong Z, Tang Z, Zhang R, Zhu J. Research progress in the heat resistance, toughening and filling modification of PLA. *Sci China Chem*. 2016;59:1355-1368.
24. Aliotta L, Cinelli P, Coltelli MB, Lazzeri A. Rigid filler toughening in PLA-Calcium Carbonate composites: effect of particle surface treatment and matrix plasticization. *Eur Polym J*. 2019;113:78-88.
25. Qian S, Sheng K. PLA toughened by bamboo cellulose nanowhiskers: role of silane compatibilization on the PLA bionanocomposite properties. *Compos Sci Technol*. 2017;148:59-69.
26. Petchwattana N, Naknaen P, Narupai B. Combination effects of reinforcing filler and impact modifier on the crystallization and toughening performances of poly(lactic acid). *Express Polym Lett*. 2020;14:848-859.
27. Krishnan S, Pandey P, Mohanty S, Nayak SK. Toughening of polylactic acid: an overview of research progress. *Polym-Plast Technol Eng*. 2015;55:1623-1652.
28. Fekete I, Ronkay F, Lendvai L. Highly toughened blends of poly(lactic acid) (PLA) and natural rubber (NR) for FDM-based 3D printing applications: the effect of composition and infill pattern. *Polym Test*. 2021;99:107205.
29. Mehrabi Mazidi M, Edalat A, Berahman R, Hosseini FS. Highly-toughened polylactide- (PLA-) based ternary blends with significantly enhanced glass transition and melt strength: tailoring the interfacial interactions, phase morphology, and performance. *Macromolecules*. 2018;51:4298-4314.
30. Chen H, Yu X, Zhou W, Peng S, Zhao X. Highly toughened polylactide (PLA) by reactive blending with novel polycaprolactone-based polyurethane (PCLU) blends. *Polym Test*. 2018;70:275-280.
31. Sanchez-Safont EL, Arrillaga A, Anakabe J, Cabedo L, Gamez-Perez J. Toughness enhancement of PHBV/TPU/cellulose compounds with reactive additives for compostable injected parts in industrial applications. *Int J Mol Sci*. 2018;19:2102.
32. Jiang J, Su L, Zhang K, Wu G. Rubber-toughened PLA blends with low thermal expansion. *J Appl Polym Sci*. 2013;128:3993-4000.
33. Yeo JCC, Lin TT, Koh JJ, et al. Insights into the nucleation and crystallization analysis of PHB-rubber toughened PLA biocomposites. *Compos Commun*. 2021;27:100894.
34. Dogan SK, Reyes EA, Rastogi S, Ozkoc G. Reactive compatibilization of PLA/TPU blends with a diisocyanate. *J Appl Polym Sci*. 2014;131:40251.
35. Kilic NT, Can BN, Kodal M, Özkoç G. Reactive compatibilization of biodegradable PLA/TPU blends via hybrid nanoparticle. *Prog Rubber Plast Recycl Technol*. 2021;37:301-326.
36. Pandey K, Antil R, Saha S, Jacob J, Balavairavan B. Poly(lactic acid)/thermoplastic polyurethane/wood flour composites: evaluation of morphology, thermal, mechanical and biodegradation properties. *Mater Res Express*. 2019;6:125306.
37. Azadi F, Jafari SH, Khonakdar HA, Arjmand M, Wagenknecht U, Altstädt V. Influence of graphene oxide on thermally induced shape memory behavior of PLA/TPU blends: correlation with morphology, creep behavior, crystallinity, and dynamic mechanical properties. *Macromol Mater Eng*. 2020;306:2000576.
38. Dogan SK, Boyacioglu S, Kodal M, Gokce O, Ozkoc G. Thermally induced shape memory behavior, enzymatic degradation and biocompatibility of PLA/TPU blends: "Effects of compatibilization". *J Mech Behav Biomed Mater*. 2017;71:349-361.
39. Datta J, Kasprzyk P. Thermoplastic polyurethanes derived from petrochemical or renewable resources: a comprehensive review. *Polym Eng Sci*. 2018;58:14-35.
40. Yao Y, Xiao M, Liu W. A short review on self-healing thermoplastic polyurethanes. *Macromol Chem Phys*. 2021;222:2100002.
41. Nofar M, Mohammadi M, Carreau PJ. Effect of TPU hard segment content on the rheological and mechanical properties of PLA/TPU blends. *J Appl Polym Sci*. 2020;137:49387.
42. Xiao J, Gao Y. The manufacture of 3D printing of medical grade TPU. *Prog Addit Manuf*. 2017;2:117-123.
43. Brancewicz-Steinmetz E, Sawicki J, Byczkowska P. The influence of 3D printing parameters on adhesion between

polylactic acid (PLA) and thermoplastic polyurethane (TPU). *Materials*. 2021;14:6464.
44. Drupitha MP, Bankoti K, Pal P, et al. Morphology-induced physico-mechanical and biological characteristics of TPU-PDMS blend scaffolds for skin tissue engineering applications. *J Biomed Mater Res B Appl Biomater*. 2019;107:1634-1644.
45. Gopalan AM, Naskar K. Ultra-high molecular weight styrenic block copolymer/TPU blends for automotive applications: influence of various compatibilizers. *Polym Adv Technol*. 2019; 30:608-619.
46. Rigotti D, Dorigato A, Pegoretti A. 3D printable thermoplastic polyurethane blends with thermal energy storage/release capabilities. *Mater Today Commun*. 2018;15:228-235.
47. Jašo V, Cvetinov M, Rakić S, Petrović ZS. Bio-plastics and elastomers from polylactic acid/thermoplastic polyurethane blends. *J Appl Polym Sci*. 2014;131:131.
48. Feng F, Ye L. Morphologies and mechanical properties of polylactide/thermoplastic polyurethane elastomer blends. *J Appl Polym Sci*. 2011;119:2778-2783.
49. Han J-J, Huang H-X. Preparation and characterization of biodegradable polylactide/thermoplastic polyurethane elastomer blends. *J Appl Polym Sci*. 2011;120:3217-3223.
50. Liu Z-W, Chou H-C, Chen S-H, et al. Mechanical and thermal properties of thermoplastic polyurethane-toughened polylactide-based nanocomposites. *Polym Compos*. 2014;35: 1744-1757.
51. Dorigato A, Sebastiani M, Pegoretti A, Fambri L. Effect of silica nanoparticles on the mechanical performances of poly(lactic acid). *J Polym Environ*. 2012;20:713-725.
52. Fambri L, Dorigato A, Pegoretti A. Role of surface-treated silica nanoparticles on the thermo-mechanical behavior of poly(lactide). *Appl Sci*. 2020;10:6731.
53. Tait M, Pegoretti A, Dorigato A, Kalaitzidou K. The effect of filler type and content and the manufacturing process on the performance of multifunctional carbon/poly-lactide composites. *Carbon*. 2011;49:4280-4290.
54. Xiu H, Huang C, Bai H, et al. Improving impact toughness of polylactide/poly(ether)urethane blends via designing the phase morphology assisted by hydrophilic silica nanoparticles. *Polymer*. 2014;55:1593-1600.
55. Xiu H, Bai HW, Huang CM, Xu CL, Li XY, Fu Q. Selective localization of titanium dioxide nanoparticles at the interface and its effect on the impact toughness of poly(L-lactide)/poly (ether)urethane blends. *Express Polym Lett*. 2013;7:261-271.
56. Ye W, Dou H, Cheng Y, Zhang D. Self-sensing properties of 3D printed continuous carbon fiber-reinforced PLA/TPU honeycomb structures during cyclic compression. *Mater Lett*. 2022; 317:132077.
57. Lin M-C, Lin J-H, Bao L. Applying TPU blends and composite carbon fibers to flexible electromagnetic-shielding fabrics: long-fiber-reinforced thermoplastics technique. *Compos A: Appl Sci Manuf*. 2020;138:106022.
58. Huang J, Liu H, Lu X, Qu J. *Thermal and Mechanical Properties of TPU/PBT Reinforced by Carbon Fiber*. Vol 1713. AIP Publishing; 2016:120003.
59. Jiang S, Li Q, Zhao Y, Wang J, Kang M. Effect of surface silanization of carbon fiber on mechanical properties of carbon fiber reinforced polyurethane composites. *Compos Sci Technol*. 2015; 110:87-94.
60. Cheng K-C, Lin Y-H, Guo W, et al. Flammability and tensile properties of polylactide nanocomposites with short carbon fibers. *J Mater Sci*. 2014;50:1605-1612.
61. Zhang Y, Zhang Y, Liu Y, Wang X, Yang B. A novel surface modification of carbon fiber for high-performance thermoplastic polyurethane composites. *Appl Surf Sci*. 2016;382:144-154.
62. Yin X, Wang L, Li S, et al. Preparation and characterization of carbon fiber/polylactic acid/thermoplastic polyurethane (CF/PLA/TPU) composites prepared by a vane mixer. *J Polym Eng*. 2017;37:355-364.
63. Qian K, Qian X, Chen Y, Zhou M. Poly(lactic acid)-thermoplastic poly(ether)urethane composites synergistically reinforced and toughened with short carbon fibers for three-dimensional printing. *J Appl Polym Sci*. 2018;135:46483.
64. Stojcevski F, Hilditch TB, Henderson LC. A comparison of interfacial testing methods and sensitivities to carbon fiber surface treatment conditions. *Compos A: Appl Sci Manuf*. 2019; 118:293-301.
65. Hassan EAM, Yang L, Elagib THH, et al. Synergistic effect of hydrogen bonding and π-π stacking in interface of CF/PEEK composites. *Compos Part B Eng*. 2019;171:70-77.
66. Liu L, Yan F, Li M, et al. Improving interfacial properties of hierarchical reinforcement carbon fibers modified by graphene oxide with different bonding types. *Compos A: Appl Sci Manuf*. 2018;107:616-625.
67. Yuan X, Zhu B, Cai X, Liu J, Qiao K, Yu J. Optimization of interfacial properties of carbon fiber/epoxy composites via a modified polyacrylate emulsion sizing. *Appl Surf Sci*. 2017;401: 414-423.
68. Yao Z, Wang C, Wang Y, et al. Effect of microstructures of carbon nanoproducts grown on carbon fibers on the interfacial properties of epoxy composites. *Langmuir*. 2022;38:2392-2400.
69. Fu J, Zhang M, Jin L, et al. Enhancing interfacial properties of carbon fibers reinforced epoxy composites via Layer-by-Layer self assembly GO/SiO2 multilayers films on carbon fibers surface. *Appl Surf Sci*. 2019;470:543-554.
70. Mahmood H, Simonini L, Dorigato A, Pegoretti A. Graphene deposition on glass fibers by triboelectrification. *Appl Sci*. 2021; 11:3123.
71. Raphael N, Namratha K, Chandrashekar BN, et al. Surface modification and grafting of carbon fibers: a route to better interface. *Prog Cryst Growth Charact Mater*. 2018;64:75-101.
72. Latif R, Wakeel S, Zaman Khan N, Noor Siddiquee A, Lal Verma S, Akhtar Khan Z. Surface treatments of plant fibers and their effects on mechanical properties of fiber-reinforced composites: a review. *J Reinf Plast Compos*. 2018;38:15-30.
73. Tiwari S, Bijwe J. Surface treatment of carbon fibers—a review. *Procedia Technol*. 2014;14:505-512.
74. Zhang G, Sun S, Yang D, Dodelet J-P, Sacher E. The surface analytical characterization of carbon fibers functionalized by H2SO4/HNO3 treatment. *Carbon*. 2008;46:196-205.
75. Tiwari S, Bijwe J, Panier S. Tribological studies on polyetherimide composites based on carbon fabric with optimized oxidation treatment. *Wear*. 2011;271:2252-2260.
76. Davachi SM, Kaffashi B. Preparation and characterization of poly L-lactide/triclosan nanoparticles for specific antibacterial and medical applications. *Int J Polym Mater Polym Biomater*. 2015;64:497-508.

77. Rahmanian S, Suraya AR, Zahari R, Zainudin ES. Synthesis of vertically aligned carbon nanotubes on carbon fiber. *Appl Surf Sci*. 2013;271:424-428.
78. Zhang Y, Zhu S, Liu Y, Yang B, Wang X. The mechanical and tribological properties of nitric acid-treated carbon fiber-reinforced polyoxymethylene composites. *J Appl Polym Sci*. 2015;15:132.
79. Hong H, Yang L, Yuan Y, et al. Preparation, rheological properties and primary cytocompatibility of TPU/PLA blends as biomedical materials. *J Wuhan Univ Technol-Mater*. 2016;31:211-218.
80. Yazdaninia A, Jafari SH, Ehsani M, Khajavi R, Khonakdar HA. An assessment on the effect of trifluoropropyl-POSS and blend composition on morphological, thermal and thermomechanical properties of PLA/TPU. *J Therm Anal Calorim*. 2019;139:279-292.
81. Tabuani D, Bellucci F, Terenzi A, Camino G. Flame retarded thermoplastic polyurethane (TPU) for cable jacketing application. *Polym Degrad Stab*. 2012;97:2594-2601.
82. Bindu P, Thomas S. Viscoelastic behavior and reinforcement mechanism in rubber nanocomposites in the vicinity of spherical nanoparticles. *J Phys Chem B*. 2013;117:12632-12648.
83. Pistor V, Ornaghi HL, Ferreira CA, Zattera AJ. Performance of poly(ethylene-co-vinyl acetate) nanocomposites using distinct clays. *J Appl Polym Sci*. 2012;125:462-470.
84. Chua PS. Dynamic mechanical analysis studies of the interphase. *Polym Compos*. 1987;8:308-313.

How to cite this article: Simonini L, Mahmood H, Dorigato A, Pegoretti A. Tailoring the physical properties of poly(lactic acid) through the addition of thermoplastic polyurethane and functionalized short carbon fibers. *Polym Compos*. 2023;44(8):4719-4733. doi:10.1002/pc.27435